JOURNAL OF MATERIALS SCIENCE **37** (2002) 615–620

Plastic deformation kinetics of fine-grained MgO in tension

DI YANG, H. CONRAD
Department of Materials Science and Engineering, North Carolina State University, Raleigh, NC 27695-7907, USA
E-mail: hans_conrad@NCSU.edu

The plastic deformation kinetics of 99.4% MgO ($d_o = 5.3\ \mu$m) was investigated at 1500°–1600°C in uniaxial tension. It was determined that the stress exponent $n \approx 1$ and the activation energy $Q = 204$ kJ/mole. Neither the present results on MgO, nor data in the literature on MgO and other oxide ceramics, can be fully explained by the models usually proposed for the plastic deformation of fine-grained oxide ceramics. The present results are however in good agreement with the model for grain boundary diffusion plastic flow recently developed by Kim, Estrin and Bush.

1. Introduction

A review of the plastic deformation kinetics of polycrystalline MgO at high homologous temperatures is given by Wilshire [1]. The results have generally been expressed in terms of the Weertman-Dorn (W-D) equation

$$\dot{\varepsilon} = \frac{A\mu b}{kT}\left(\frac{\sigma}{\mu}\right)^n \left(\frac{b}{d}\right)^p D \tag{1}$$

where $\dot{\varepsilon}$ is the strain rate, μ the shear modulus, b the Burgers vector, σ the applied stress, d the grain size and $D = D_o \exp(-Q/RT)$ the appropriate diffusion constant. A, n, p, D_o and Q are constants which define the rate-controlling process, and kT has its usual meaning. The values listed by Wilshire for the constants in Equation 1 determined in creep tests on polycrystalline MgO at 1273–1800 K are $n = 1.0$–3.5, $p = 2.0$–2.5 and $Q = 192$–475 kJ/mole. This range in values suggests that different mechanisms may operate in different material and/or testing conditions. Regarding the latter, the listed tests were all creep tests in either torsion, bending or compression. *None were in uniaxial tension at a constant strain rate*. The objectives of the present investigation were therefore two-fold: (a) to determine the plastic deformation kinetics of fine-grained MgO in constant strain rate, uniaxial tension tests and (b) to identify the rate-controlling mechanism. An important innovation in carrying out the tension tests was the preparation of specimens without expensive machining.

2. Procedure

The starting material was chemical grade 99.37 wt% MgO powder with particle size $\leq 1\ \mu$m purchased from Fisher Scientific. The major given nominal impurities were 0.014% NH_4OH, 0.01% Ca and 0.1% Na; all others were <0.01%. Tensile specimens were prepared by pouring the powder into the specially designed, stainless steel die shown in Fig. 1, which had been previously constructed and employed to prepare 3YTZP [2] and Al_2O_3 [3, 4] tensile specimens. With this fixture we are able to prepare final-shaped ceramic tensile specimens quickly and economically without expensive machining.

The MgO powder was heated for 1 hr at 100°C just prior to pouring it into the die. It was then cold pressed at 70 MPa with the conforming stainless steel punch to give the tensile specimen shape shown in Fig. 1. The compacted specimen was carefully removed from the die and sintered in a two-step process: (a) it was first heated at a rate of 5°C per minute to 1000°C and held for 2 hr at this temperature and (b) it was then heated at the same rate to 1640°C and held for 2 hr at this temperature, following which it was slowly cooled to room temperature. The final form and dimensions of the specimens are shown in Fig. 2. Their density was 98% determined by the Archimedes method and the mean linear intercept grain size was 5.3 μm. A typical microstructure is given in Fig. 3a; the grain size distribution is given in Fig. 3b.

Tensile tests were performed in air at 1500°, 1550° and 1600° ±1°C employing the grip and furnace assembly shown in Fig. 2. The tests were conducted in an Instron machine at a constant crosshead speed. The plastic strain was determined from the crosshead displacement with correction for the spring constant of the machine-grip assembly. True stresses and strains were calculated from the specimen elongations in the usual manner. The final elongations taken from crosshead displacements agreed with measurements on the fractured specimens. Both tests at a constant crosshead speed throughout (with a strain rate $\dot{\varepsilon} \approx 10^{-4}\ s^{-1}$) and with strain rate cycling (alternately changing the crosshead speed by a factor of 2) were conducted. The latter type of tests provided the value of the stress exponent $n = \partial \ln \dot{\varepsilon} / \partial \ln \sigma$ at constant structure.

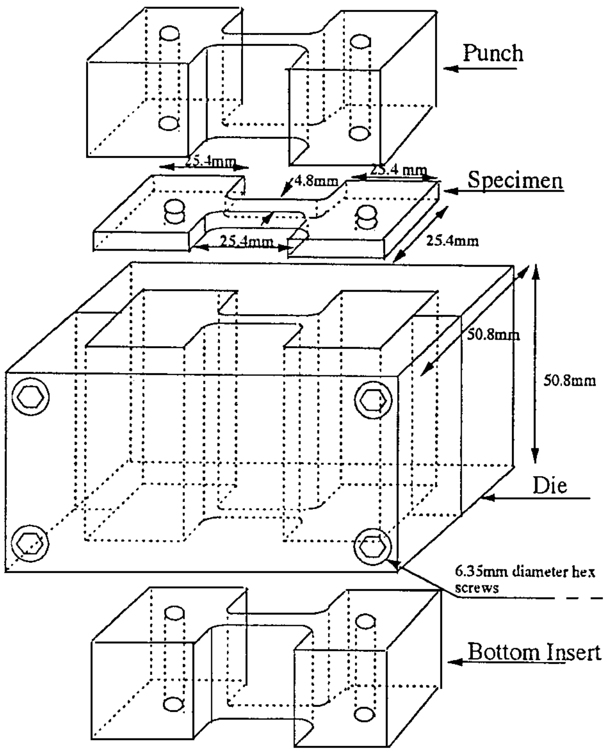

Figure 1 Schematic of punch-die fixture employed to prepare the tensile specimens.

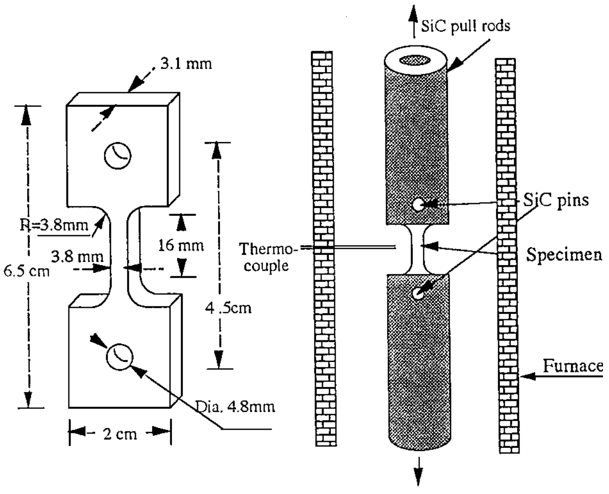

Figure 2 Form and dimensions of the tensile specimens and the grip assembly.

3. Results

True stress-true strain curves obtained in the constant crosshead speed tests are presented in Fig. 4. In keeping with usual behavior the flow stress decreases with temperature and the elongation increases, the latter being 24% (engineering total elongation) at 1500°C and 32% at 1600°C. Because of the soft spring constant of the present machine-grip assembly and the small value of the stress exponent n (to be established below), the strain hardening indicated in Fig. 4 (especially for $\varepsilon \leq 0.05$) results to some degree from the increase in plastic strain rate with initial straining as the specimen is loaded with a constant crosshead speed.

Stress-strain behavior in the strain rate cycling tests is illustrated in Fig. 5. Included is the value of the stress exponent $n = \log(\dot{\varepsilon}_2/\dot{\varepsilon}_1)/\log(\sigma_2/\sigma_1)$ determined from the change in flow stress which resulted from a change in strain rate. It is seen that $n \approx 1$, relatively independent of strain. A value of $n \approx 1$ was also obtained at the other two temperatures; see Fig. 6. A value of $n \approx 1$ has been reported for the creep of polycrystalline MgO tested in bending at 1107°–1527°C [1, 5–7].

Taking $n = 1$, rearrangement of Equation 1 gives

$$\ln\left(\frac{\sigma}{T}\right) = \ln\left[\frac{\dot{\varepsilon}k}{AbD_o}\left(\frac{d}{b}\right)^p\right] + \frac{Q}{RT} \qquad (2)$$

The value of the activation energy Q can then be obtained from the temperature dependence of the flow stress by plotting log (σ/T) vs. $1/T$ and assuming that the other parameters are independent of temperature. Such plots are given in Fig. 7 for $\varepsilon = 0.05$, 0.10 and 0.20, which strains are in the range where the apparent rate of strain hardening and its temperature dependence are relatively small, suggesting an approximately constant structure at a constant strain. The least squares values of the intercepts and slopes of the straight lines in Fig. 7 are:

ε	Intercept	Slope = $Q/2.3\ R$	Q (kJ/mole)
0.05	7.80×10^{-3}	2.48×10^4	206
0.10	8.69×10^{-3}	2.48×10^4	206
0.20	15.19×10^{-3}	2.40×10^4	200
	10.56×10^{-3} Avg.		204 Avg.

The values of Q determined from the slopes are in agreement with the lowest values (192–226 kJ/mole) which have been reported for the creep of polycrystalline MgO [1, 5, 8]. Of significance is that they are in accord with the value (200 kJ/mole) for Mg^{2+} *grain boundary* diffusion in MgO [9]. For comparison, the value of Q for O^{2-} grain boundary diffusion is 230 kJ/mole, that for extrinsic cation lattice diffusion is 266 kJ/mole and that for extrinsic anion lattice diffusion is 261 kJ/mole [9].

4. Discussion

Of interest is the process or mechanism responsible for the plastic deformation of MgO in the present tests. As indicated above, the derived activation energy Q is in accord with grain boundary diffusion as the rate-controlling step. The experimental value of the stress exponent $n \approx 1$ is in accord with the following four deformation processes: (a) diffusion flow (Nabarro-Herring [10, 11], Coble [12], or Kim-Estrin-Bush [13]), (b) grain boundary shear (Conrad-Narayan [13]), (c) grain boundary sliding accommodated by diffusion flow (Raj-Ashby [15]) and (d) low stress dislocation motion (Harper-Dorn [16, 17]). The constitutive equations which describe these deformation modes are given in Table I. Of these, the two original diffusion flow

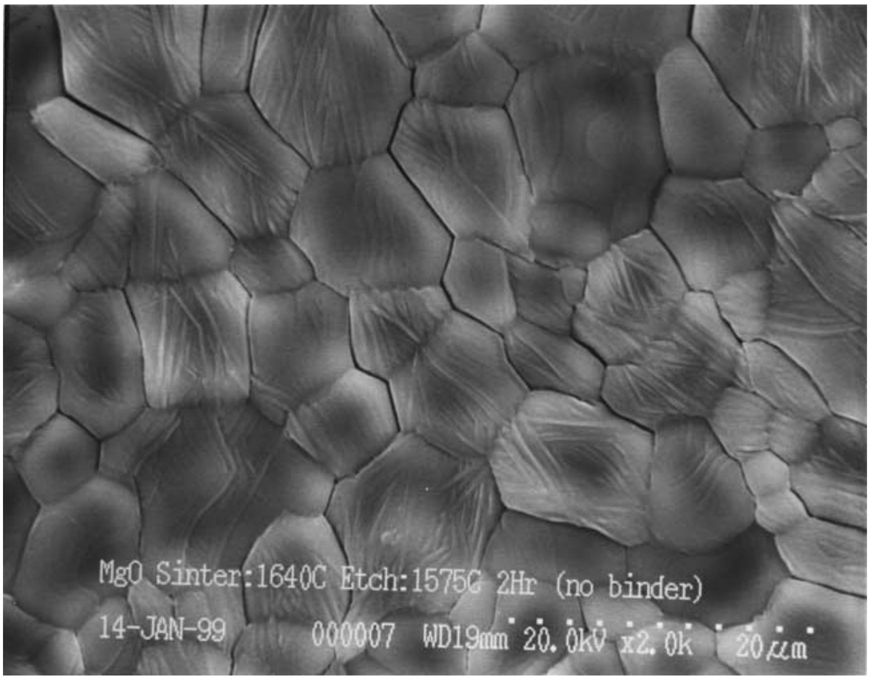

(a)

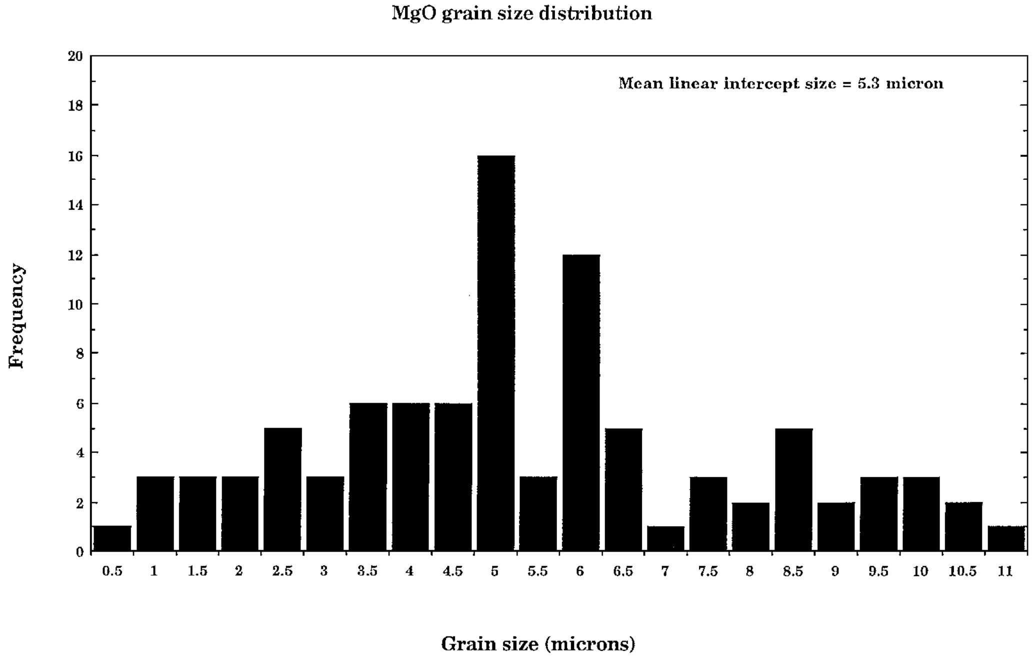

(b)

Figure 3 (a) SEM micrograph of sintered and etched (2 hr at 1575°C) MgO specimen. (b) Grain size distribution.

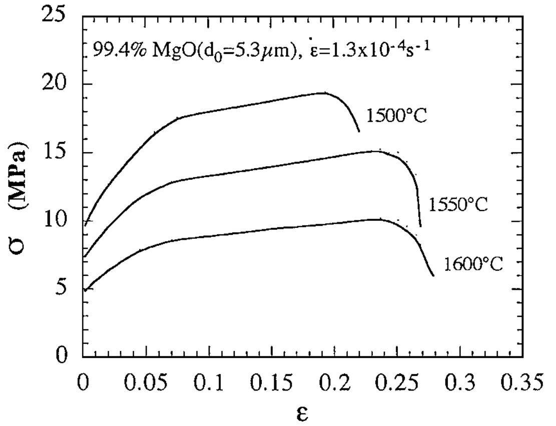

Figure 4 True stress vs. true strain curves at 1500°, 1550°, and 1600°C.

models (i.e. the Nabarro-Herring and Coble models) have been most frequently considered to apply to the deformation of fine-grained ceramics at low stresses.

To ascertain which of the models listed in Table I best describes the present results, the experimental values of the quantity $\dot{\varepsilon}T/\sigma$ are compared in Table II with those predicted by each model, considering the diffusion of each ion species as the possible rate-controlling step. The underlined value in Table II is that for the slowest ion in the specific model or process. This meets the requirements that stoichiometry or charge neutrality be maintained and that no local variation in composition exists. Fig. 8 illustrates the importance of these requirements when deciding between N—H and Coble diffusion flow as the major deformation process in MgO with

TABLE I Constitutive equations for plastic deformation mechanisms with $n = 1$

Model	Equation	
Nabarro-Herring (N-H)	$\dot{\varepsilon}_{\text{N-H}} = A_{\text{N-H}} D_v \Omega \sigma / d^2 kT$	(1)
Coble (C)	$\dot{\varepsilon}_{\text{C}} = A_{\text{C}} \delta D_b \Omega \sigma / d^3 kT$	(2)
Kim-Estrin-Bush (K-E-B)	$\dot{\varepsilon}_{\text{K-E-B}} = 2 D_b \Omega \sigma / d^2 kT$	(3)
Raj-Ashby (R-A)	$\dot{\varepsilon}_{\text{R-A}} = \delta D_b \Omega \sigma / h^2 dkT$	(4)
Conrad-Narayan (C-N)	$\dot{\varepsilon}_{\text{C-N}} = 2 \delta D_b \Omega \sigma \nu_D / dkT$	(5)
Harper-Dorn (H-D)	$\dot{\varepsilon}_{\text{H-D}} = A_{\text{H-D}} D_v b \sigma / kT$	(6)

$A_{\text{H-N}} = 27$ and $A_{\text{C}} = 54$ [18]; $A_{\text{H-D}} = \rho_m \Omega / b \approx 10^{-9}$ [9], with ρ_m = mobile dislocation denisity.

D_v and D_b = lattice and grain boundary diffusion coefficients, respectively.

Ω = atomic volume; b = Burgers vector; d = grain size; δ = grain boundary width; h = height of grain boundary serrations; ν_D = Debye frequency.

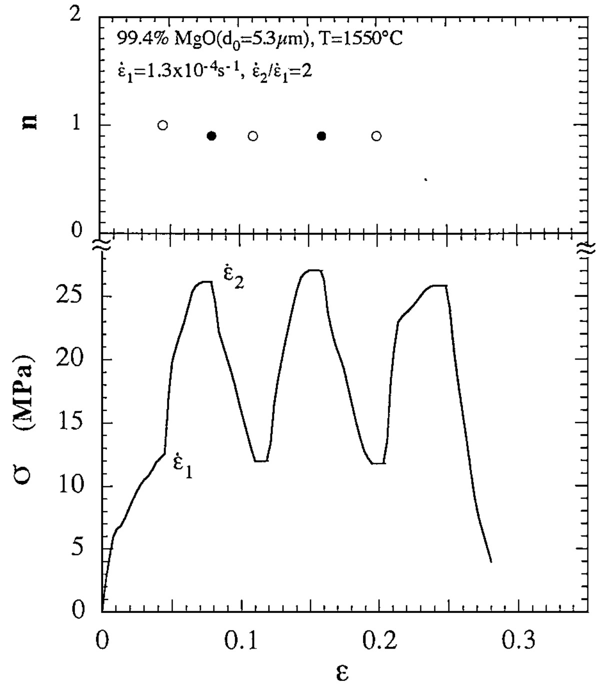

Figure 5 Stress-strain behavior in the strain rate cycling tests at 1550°C. Included are the values of $n = \log(\dot{\varepsilon}_2/\dot{\varepsilon}_1)/\log(\sigma_2/\sigma_1)$ Open symbols are for increases in strain rate; filled are for decreases in rate.

$d_o = 5.3$ μm. It is here seen that if we consider *only* the diffusion of the Mg^{2+} ions, the Nabarro-Herring (N-H) process gives a higher strain rate than the Coble process. In contrast, if we *only* consider the O^{2-} ions, the Coble process gives the higher rate. Thus, to maintain stoichiometry and prevent local variation in N-H diffusional flow is controlled by the slower moving O^{2-} ions through the *lattice* and Coble flow by the slower moving Mg^{2+} ions along the *grain boundaries*. The end result of this analysis is that Coble diffusion flow is the faster of the two processes, and grain boundary diffusion of the Mg^{2+} ions is the rate-controlling step. The strain rate is thus detemined by the slower moving ion in the faster process.

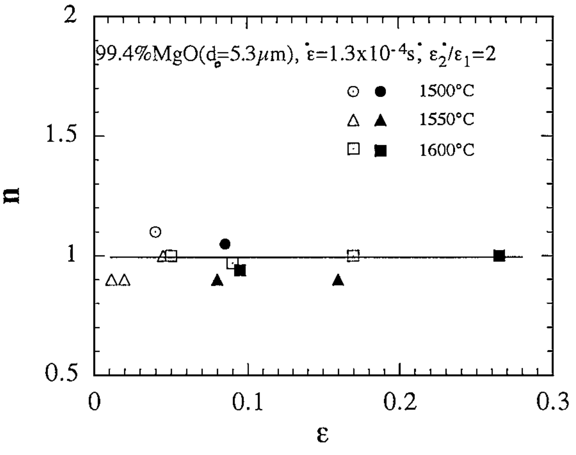

Figure 6 Stress exponent n vs. strain at 1500°, 1550°, and 1600°C.

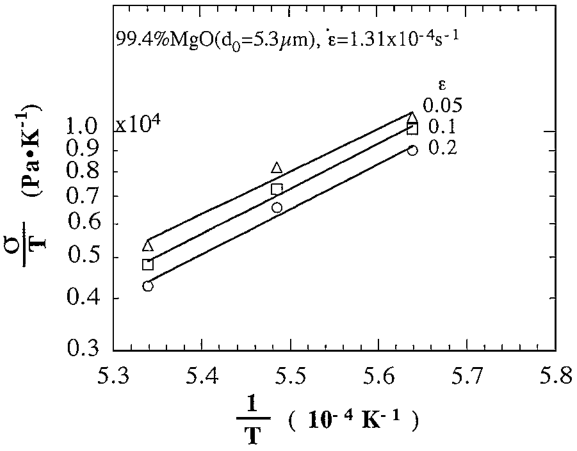

Figure 7 $\log(\sigma/T)$ vs. $1/T$ for three strains.

As mentioned above, the deformation of fine-grained ceramics has been most frequently considered to occur by diffusion flow. However, we note from Table II that the present experimental values of $\dot{\varepsilon}T/\sigma$ are 3 to 4 orders of magnitude larger than those predicted by the N-H and Coble models. A similar situation exists for ceramics in general (e.g., Al_2O_3 [19, 20], ZrO_2 [21] and UO_2 [22]) in that the experiential strain rate is orders

TABLE II Comparison of predicted values of $\dot{\varepsilon}T/\sigma$ (K/Pa-s) with experiment[a]

						Harper-Dorn[b]			
T(K)	Ion	Nabarro-Herring	Coble	Raj-Ashby	Conrad-Narayan	D_v	D_c	Kim-Estrin-Bush	Experimental
1773	Mg^{+2}	7.8×10^{-10}	$\underline{1.9 \times 10^{-11}}$	$\underline{1.0 \times 10^{-23}/h^2}$	$\underline{1.9 \times 10^{-10}}$	1.2×10^{-11}	$\underline{2.7 \times 10^{-9}}$	$\underline{1.3 \times 10^{-8}}$	1.38×10^{-8}
	O^{-2}	$\underline{6.5 \times 10^{-12}}$	1.1×10^{-10}	$5.5 \times 10^{-22}/h^2$	1.1×10^{-9}	$\underline{1.1 \times 10^{-13}}$	1.5×10^{-8}	7.3×10^{-8}	
1873	Mg^{+2}	2.0×10^{-9}	$\underline{3.8 \times 10^{-11}}$	$\underline{2.0 \times 10^{-23}/h^2}$	$\underline{4.0 \times 10^{-10}}$	3.2×10^{-11}	$\underline{5.6 \times 10^{-9}}$	$\underline{2.5 \times 10^{-8}}$	2.80×10^{-8}
	O^{-2}	$\underline{1.7 \times 10^{-11}}$	2.6×10^{-10}	$1.4 \times 10^{-22}/h^2$	2.7×10^{-9}	$\underline{2.8 \times 10^{-13}}$	3.6×10^{-8}	1.7×10^{-7}	

[a] Values of D_v, δD_b, Ω taken from [9]; $\nu_D = 10^{13}$ s^{-1}.

[b] $A_{\text{H-D}} = 10^{-9}$; D_v = lattice diffusion; D_c = dislocation core diffusion.

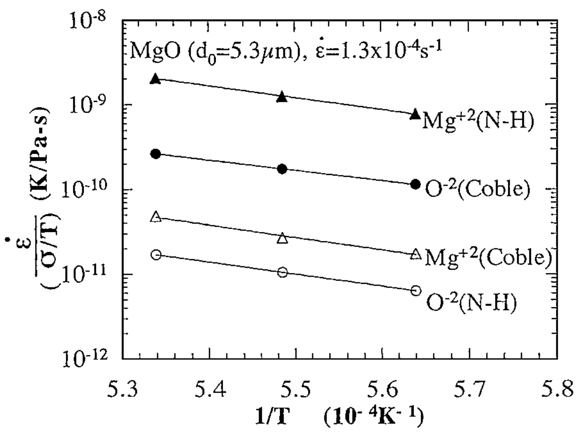

Figure 8 log(σ/T) vs. $1/T$ for Nabarro-Herring (N-H) and Coble creep of MgO ($d = 5.3$ μm) when the rate-controlling process is the diffusion of either the anion or cation. Diffusion and other coefficients taken from [9].

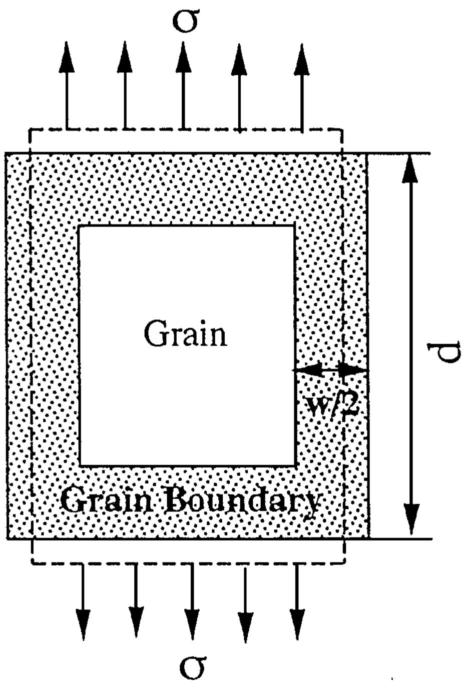

Figure 9 Schematic of the model for the deformation of the grain boundary phase by Kim *et al.* [13].

of magnitude higher than predicted by the diffusion flow models, even though the constants n, p, and Q of Equation 1 have the proper values. Also, the creep rate of fine-grained metals is in general significantly larger than predicted by the N-H and Coble diffusion models [23]. Thus, usually neither the N-H nor the Coble diffusion models accurately predict the strain rate for the conditions where they are expected to apply, including the present results on MgO. Kim *et al.* [13] have recently developed an equation for grain boundary diffusion plastic flow (Fig. 9 and Equation 3 in Table I) which differs from that of Coble in that the strain rate does not depend on grain boundary width w and varies with d^{-2} rather than d^{-3}. We see in Table II that the values of $\dot{\varepsilon}T/\sigma$ predicted by the K-E-B equation for the present material and test conditions are in excellent agreement with the experimental values. This strongly suggests that the major plastic deformation process in the present tests is grain boundary diffusion flow.

An alternative model is grain boundary sliding accommodated by diffusion flow developed by Raj and Ashby [15], which is given by Equation 4 in Table I. The unknown factor in this model is the periodic grain boundary serration or projection height h. Inserting the experimental value of $\dot{\varepsilon}T/\sigma$ into Equation 4 of Table I gives $h \approx 100b$, which is not unreasonable. However, since the reported dependence of the creep rate on grain size often varies with d^{-n}, where $n = 2$–3, full agreement of experiment with the R-A model given by Equation 4 in Table I requires that h^2 increase with grain size. A variation of h with grain size could conceivably occur if the serrations in the boundary resulted from either grain boundary migration or from emission or absorption of dislocations at the boundary. This could conceivably occur during the initial strain hardening at $\varepsilon < 0.05$ in Fig. 4.

It is also seen from Table II that the experimental values of $\dot{\varepsilon}T/\sigma$ are two orders of magnitude larger than predicted by the Conrad-Narayan (C-N) grain boundary shear model and five orders of magnitude larger than predicted by the Harper-Dorn (H-D) dislocation model based on lattice diffusion. For the C-N model to agree with the present experimental results would require that the shear stain produced by a single ion jump be 100 times larger than an atomic distance and that the multiplying factor be proportional to d^{-1}. The large strain could result from a cascading effect, but the details would need further development.

Regarding the H-D model, by assuming that dislocation core diffusion is the rate-controlling step rather that lattice diffusion, the predicted values of $\dot{\varepsilon}T/\sigma$ come within a factor of five of the experimental value. This is now within the accuracy of the diffusion data. However, to account for the generally observed effect of grain size on the strain rate of fine grained ceramics, the mobile dislocation density would need to have an inverse dependence on grain size. Again, this would need further investigation.

The above thus indicates that good agreement between the present experimental results on fine-grained MgO at 1500°–1600°C and predictions only exists for the grain boundary diffusion plastic flow model recently developed by Kim *et al.* [13]. The other models considered either predict strain rates that are too low by orders of magnitude or would require further development to give a fit between theory and experiment. It should however be pointed out that the agreement with the Kim-Estrin-Bush model exists for the grain size and size distribution in the present material. Whether the model applies to other grain sizes and distributions needs further investigation.

5. Summary and conclusions

1. The plastic deformation kinetics of polycrystalline 99.4% MgO ($d_o = 5.3\mu$m) was determined at 1500°–1600°C employing constant strain rate, uniaxial tension tests. The specimens exhibited total elongations of 24–32%.

2. A special die and procedure are described by which the tensile specimens were prepared quickly and economically.

3. It was determined that the stress exponent $n \approx 1$ and the activation energy $Q = 204 \pm 4$ kJ/mole for the plastic deformation of the present material.

4. The present experiment results are in good agreement with the grain boundary diffusion plastic flow model recently developed by Kim, Estrin and Bush.

Acknowledgements

This research was funded by the U.S. Army Research Office under Grant No. DAAH04-94G-0311 with Dr. W. Simmons as technical monitor. The authors also wish to thank Dr. Y. Fahmy for taking the SEM micrographs and making the grain size measurements.

References

1. B. WILSHIRE, *British Ceramic Trans.* **94** (1995) 57.
2. DI YANG and H. CONRAD, *Scripta Mater.* **36** (1997) 1431.
3. *Idem.*, *ibid.* **41** (1999) 397.
4. J. CAMPBELL, Y. FAHMY and H. CONRAD, *Met. Mater. Trans. A.* **30A** (1999) 2817.; *Idem.*, *ibid.* **30A** (1999) 2817.
5. E. PASSMORE, R. DUFF and T. VASILOS, *J. Am. Ceram.* 49 (1966) 594.
6. H. TAGAI and T. ZISNER, *ibid.* **51** (1968) 303.
7. G. TERWILLIGER, H. BOWEN and R. GORDON, *ibid.* **53** (1970) 241.
8. T. ZISNER and H. TAGAI, *ibid.* **51** (1968) 310.
9. H. J. FROST and M. F. ASHBY, "Deformation-Mechanism Maps" (Pergamon Press, New York, 1982) p. 84.
10. F. R. N. NABARRO, in "Report on a Conference on the Strength of Metals" (Phys. Soc., London, 1948) p. 75.
11. C. HERRING, *J. Appl. Phys.* **21** (1950) 437.
12. R. L. COBLE, *ibid.* **34** (1963) 1679.
13. H. S. KIM, Y. ESTRIN and M. B. BUSH, *Acta Mater.* **48** (2000) 493.
14. H. CONRAD and J. NARAYAN, *Scripta Mater.* **42** (2000) 1025.
15. R. RAJ and M. F. ASHBY, *Metall. Trans.* **2** (1971) 1113.
16. J. HARPER and J. DORN, *Acta Mater.* **5** (1957) 654.
17. J. HARPER, L. SHEPARD and J. DORN, *ibid.* **6** (1958) 509.
18. S. R. SHAH and A. H. CHOKSHI, *Colloids and Surfaces* **A133** (1998) 57.
19. K. VENKATACHARI and R. RAJ, *J. Am. Ceram.* **69** (1986) 135.
20. A. XU and A. SOLOMON, *ibid.* **75** (1992) 985.
21. D. DIMOS and D. KOHLSTADT, *ibid.* **70** (1987) 531.
22. O. RUANO, J. WOLFENSTINE, J. WADSWORTH and O. SHERBY, *Acta Met. Mater.* **39** (1991) 661.
23. J. WADSWORTH, O. RUANO and O. SHERBY, in "Creep Behavior of Advanced Materials for the 21st Century," edited by R. Mishra, A. Mukherjee and K. Murty (TMS, Warrendale, PA, 1999) p. 425.

Received 12 September 2000
and accepted 13 June 2001